THE JOURNAL OF PHYSICAL CHEMISTRY C

Article

Cite This: J. Phys. Chem. C 2018, 122, 12819−12830

pubs.acs.org/JPCC

Effect of Halide Anions on the Structure and Dynamics of Water Next to an Alumina (0001) Surface

Aashish Tuladhar, Stefan M. Piontek, Laszlo Frazer, and Eric Borguet*

Department of Chemistry, Temple University, 1901 N. 13th Street, Philadelphia, Pennsylvania 19122, United States

Supporting Information

ABSTRACT: While ions are known to perturb hydrogen bonding networks in bulk water, our understanding of such effects is less developed for interfaces. Alumina/water interfaces are highly ordered due to strong hydrogen bonding interactions between interfacial water molecules and adjacent aluminol groups. However, how ions alter this interaction is not yet known. Herein, to address the effect of sodium halide salts on the hydrogen bonding environment of interfacial water, we investigated charged alumina (0001) surfaces using steady-state and time-resolved vibrational sum frequency generation (vSFG) spectroscopy. Our results indicate that the effect of halide anions on the attenuation of the vSFG signal next to positively and negatively charged alumina surfaces followed the sequence $F^- \gg Br^- > Cl^- > I^-$ (slightly varied direct Hofmeister series) and $Br^- > I^- \approx Cl^- > F^-$ (slightly varied indirect Hofmeister series), respectively. Additionally, time-resolved vSFG reveals that only F^- perturbs the vibrational lifetime of water next to a positively charged alumina surface by presumably breaking the strong hydrogen bonding interaction between the surface aluminol groups and the nearby water molecules.

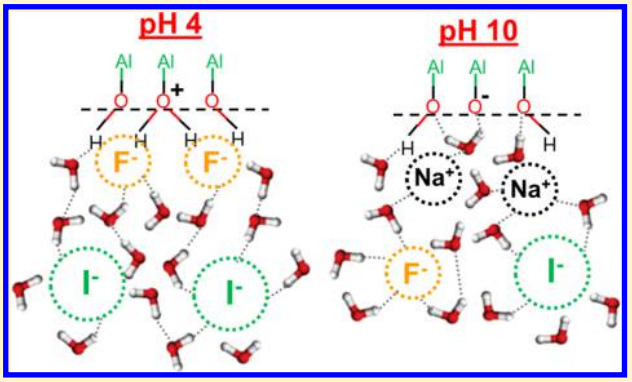

1. INTRODUCTION

Mineral−electrolyte solution interfaces are ubiquitous in geological, biological, and industrial processes, and therefore extensive research is dedicated to understanding the macro- and microscopic properties of such environments. Mineral dissolution, a macroscopic property that is largely dependent on the solution environment (pH, ionic strength, and electrolyte) is responsible for many geochemical phenomena, e.g., transportation and sequestration of CO_2 and contaminants, soil fertility, rock weathering, and the formation of ore deposits. Only recently was experimental evidence linking the interfacial solvent structure, a microscopic property, with mineral dissolution acquired.[1,2] Therefore, it is critical to obtain molecular level insight on how ions affect the interaction between the mineral surface and the aqueous solvent to understand the physical chemistry of the mineral−electrolyte solution interface.

The point of zero charge (PZC) of the α-Al_2O_3(0001), a geologically[3,4] and technologically[5−10] important mineral, is around neutral pH. Hence, alumina provides an opportunity to investigate the effect of ions next to both positively and negatively charged surfaces. Our previous studies revealed that the water next to alumina surfaces is strongly hydrogen bonded, resulting in its vibrational dynamics being faster than that of bulk water.[11,12] Moreover, the presence of NaCl, up to 0.1 M in bulk solution, seems to have little to no effect on the vibrational dynamics of the alumina/water interface.[11,12]

Specific ion effects at the alumina/water interface have been extensively investigated using various approaches, e.g., streaming potential,[13,14] electrophoresis,[15] adsorption isotherm,[16−18] electroacoustic,[19,20] and theoretical simulations.[21−27] The general rule of thumb for the adsorption affinity of cations toward metal oxides is: for high dielectric constant (ε), in oxides (like α-TiO_2, ε = 121[26]), cation interfacial affinity decreases with size ($Li^+ > Na^+ > K^+ > Rb^+ > Cs^+$).[21,26,27] This behavior is also known as an indirect Hofmeister series. In contrast, for low dielectric constant oxides (like α-SiO_2, ε = 4.6[26]), cation affinity increases with size ($Cs^+ > Rb^+ > K^+ > Na^+ > Li^+$); showing direct Hofmeister series behavior.[21,26,27] Furthermore, for intermediate dielectric constant oxides such as α-Al_2O_3 (ε = 10.4), all metal cations were predicted to adsorb to similar extent.[26] However, most experimental[13−15,19,20] and theoretical[22,24,25] studies observed some kind of cation specificity generally in line with the indirect Hofmeister series.

Anion specificity on alumina surfaces has also been investigated experimentally,[14,15,17−20] but whether the specific anion effect follows the direct or indirect Hofmeister series is not clear. Theoretically, relative anion adsorption on alumina surface was suggested to follow the direct Hofmeister series by Sahai,[25] whereas studies by Sverjensky[26] and Piasecki et al.[21]

Received: March 29, 2018
Revised: May 21, 2018
Published: June 12, 2018

DOI: 10.1021/acs.jpcc.8b03004
J. Phys. Chem. C 2018, 122, 12819−12830

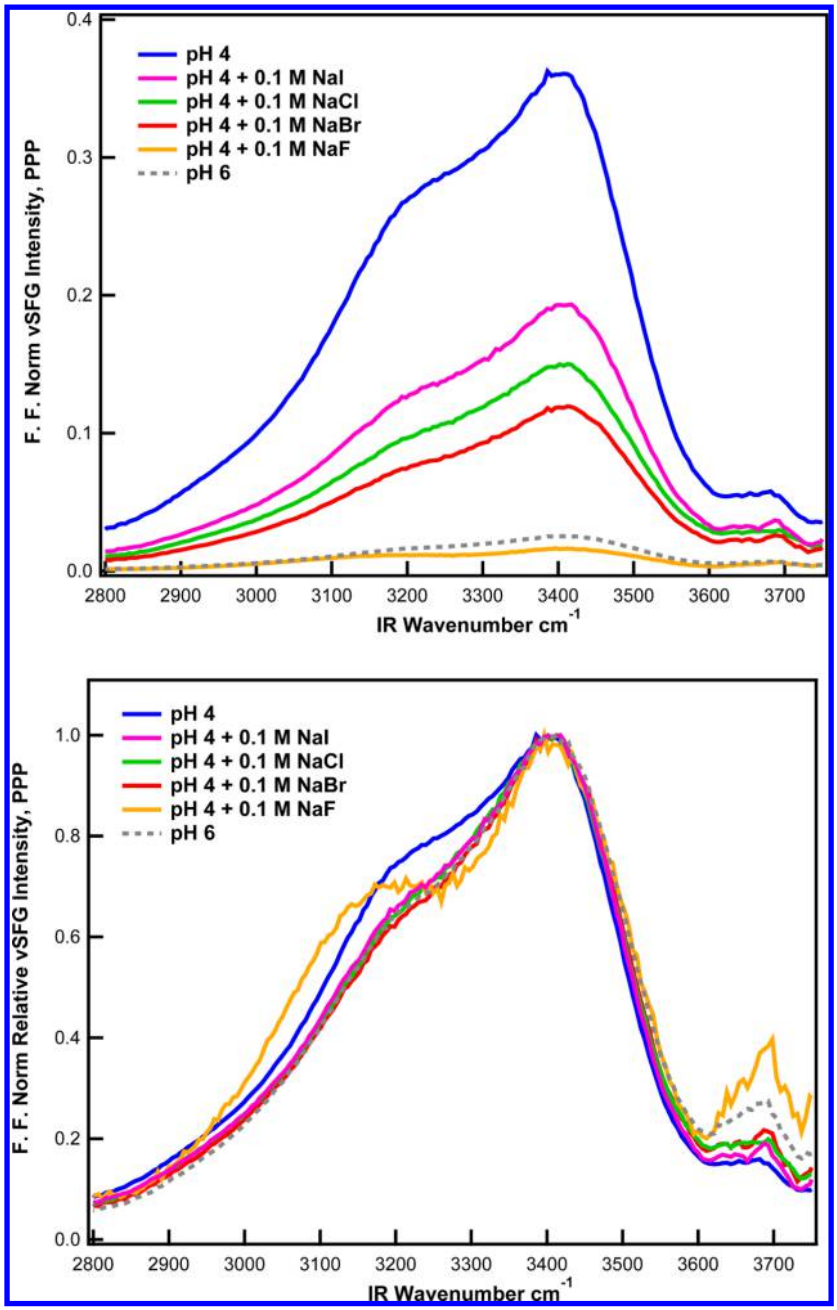

Figure 1. Effect of halide salts on the PPP-vSFG spectra of the α-$Al_2O_3(0001)/H_2O$ (pH 4) interface. The gray dotted line represents the vSFG spectra at pH 6, which is the PZC, i.e., net neutral surface charge. The colored solid lines represent the vSFG spectra at pH 4, where the surface is positively charged without excess salt (blue) and with 0.1 M NaF (yellow), NaCl (green), NaBr (red), and NaI (pink). The top figure compares the absolute intensity of different solutions, whereas the bottom figure has been normalized to the maximum peak to compare the relative intensities of different peaks. All data have been normalized with respect to the infrared (IR) pulse profile and corrected for the wavelength dependence of the Fresnel factors (abbreviated FF), as described elsewhere.[11,12,72]

showed that the halide anions affinity for alumina surfaces followed a modified direct sequence ($F^- \gg I^- > Cl^- \approx Br^-$). It is important to note that the crystallographic orientation of the alumina surface was not taken into account in any of the above studies. The significance of crystallographic orientation of alumina on the anion specificity is clear from Lützenkirchen's streaming potential experiments[14] where no anion sensitivity was observed for the r-cut ($01\bar{1}2$ face), while indirect Hofmeister series behavior was observed for negatively charged c-cut (0001 face). However, the anions investigated by Lützenkirchen were Cl^-, NO_3^-, BrO_3^-, and ClO_4^-, whereas monovalent anions such as F^-, Br^-, and I^- were not investigated.

Because of the inconsistencies in the ranking of ion adsorption next to most solid surfaces, newer studies have focused on investigating the role that the physical properties (polarity and surface charge) of a surface play pertaining to the Hofmeister series.[28−31] These studies showed that the specific anion effect on the stability of a colloidal solution was reversed when the surface charge of the particle was inverted.[28−30] So it is evident that the state of the interface is critical when studying the specific ion effects. Therefore, if we are to understand the specific ion effects at the alumina surface, a systematic study

DOI: 10.1021/acs.jpcc.8b03004
J. Phys. Chem. C 2018, 122, 12819−12830

with known crystallographic orientation and surface charge needs to be performed.

Vibrational sum frequency generation (vSFG) spectroscopy is a second-order nonlinear optical technique. Hence, in the dipole approximation, centrosymmetric materials (e.g., bulk water) will not generate any sum frequency signal. However, at any interface, centrosymmetry is inherently broken, thereby making vSFG spectroscopy an intrinsically interface specific technique. Indeed, vSFG spectroscopy has been shown to be an excellent tool for investigating the structure of water next to surfaces of varying polarities (hydrophobic[32−35] vs hydrophilic[2,36−38]) and surface charge[11,12,36,39−42] (positive vs neutral vs negative). The effect of ions on the structure of interfacial water with relevance to the Hofmeister effect has also been probed using vSFG spectroscopy.[32,33,35−38,43,44] The Cremer group investigated the effect of anions next to a hydrophobic macromolecule at the air/water interface and observed that the propensity of anions to orient the interfacial water and its correlation with the Hofmeister series depended on the surface charge of the macromolecule.[32−34] Another study showed that the effect of cations on the interfacial water structure next to a negatively charged hydrophobic interface also followed the Hofmeister series.[35] Similarly, both cations and anions have been shown to affect the structure of water next to hydrophilic surfaces (SiO_2, CaF_2, and TiO_2) in accordance with the Hofmeister effect.[36−38] However, these studies on metal oxide surfaces did not investigate the ion specificity as a function of the sign of the surface charge (i.e., positive vs negative surfaces).

In the vSFG studies mentioned above, the Hofmeister ranking was deduced from the relative attenuation of the vSFG signal in the presence of ions, although the cause of the attenuation was not clearly explained.[32−36,38] In most of the previous vSFG[36,39−41,45,46] and second harmonic generation (SHG)[47−51] studies of charged surfaces, whenever ions are added to the bulk solution and a change in the vSFG and SHG signal is observed, this change is mostly attributed to the screening of surface charge by the ions. However, recent studies have shown that ions can also rearrange the interfacial water hydrogen bonding environment, resulting in a change of the vSFG spectra.[2,37,52] Therefore, with careful analysis of the vSFG signal, it should be possible to understand how ions interact with a charged surface and how this interaction affects the structure of interfacial water, which in turn should help with the better understanding of the Hofmeister effect at interfaces.

Herein, we investigate the effect of halide salts (NaF, NaCl, NaBr, and NaI) on the structure of water next to positively and negatively charged alumina (0001) surfaces using vSFG spectroscopy. Our steady-state vSFG results clearly show that the vSFG signal next to positively and negatively charged alumina surfaces follows direct and indirect Hofmeister series (with small variations), respectively, in the presence of halide salts. In addition to the steady-state vSFG experiments, we have also performed time-resolved vSFG experiments measuring the vibrational lifetime of the O−H stretch, which has been shown to be a sensitive probe of the ion effect on the hydrogen bonding environment.[11,12,53−57] Our time-resolved vSFG experiments reveal that the larger halide anions (Cl^-, I^-, and Br^-) do not alter the vibrational dynamics of the interfacial water next to positively charged alumina surfaces. In contrast, the smaller anion (F^-) slows down the vibrational dynamics of interfacial water, presumably by preferably adsorbing onto the positively charged alumina surface and disrupting the strong interaction between the water molecules and the alumina surface. This distinct interaction between alumina surfaces and F^- is probably why alumina is used as a sorbent for fluoride removal.[58−61] Furthermore, the vibrational dynamics of interfacial water next to a negatively charged alumina surface is different from the positively charged alumina surface and the presence of halide salts affect the vibrational relaxation kinetics in a unique manner.

2. EXPERIMENTAL SECTION

The sample preparation and the optical setup are described in detail in Section 1 of the Supporting Information (SI).

3. RESULTS AND DISCUSSION

3.1. Steady-State vSFG Study of Positively Charged α-Al_2O_3(0001)/H_2O Interface (pH 4). *3.1.1. Spectral Assignment and Surface Charging of Positively Charged α-Al_2O_3(0001)/H_2O Interface.* The α-Al_2O_3(0001) surface is terminated by Al_2−OH functional groups, which undergo a protonation reaction in acidic solution to form Al_2−OH_2^+ and hence a positively charged surface.[62] The vSFG spectra of the O−H stretch at the α-Al_2O_3(0001)/H_2O (pH 4) interface (Figure 1) consists of two main peaks centered at approximately 3200 and 3400 cm^{-1}, assigned to strongly and weakly hydrogen bonded O−H stretches, respectively. The origin/assignment of these O−H stretches (H_2O or Al_2OH) is still controversial but a recent theoretical study assigned the 3200 cm^{-1} peak to be mainly due to the O−H stretch of water, whereas the 3400 cm^{-1} peak was mainly due to the O−H stretch of Al−OH groups on the surface.[63] Moreover, we find good agreement between our experimental vSFG spectra and the simulated vSFG spectra[63] for neutral pH condition, i.e., the ratio between 3400 cm^{-1} peak and 3200 cm^{-1} peak from our experiments is ∼1.6, close to the theoretical ratio[63] of 1.37. However, the accurate assignment of the O−H stretching region is complicated by the strong inter- and intramolecular vibrational couplings (e.g., a Fermi resonance between the O−H stretch and the overtone of the water bend), as observed in other interfaces, e.g., silica/water[64] and air/water.[65] A smaller peak at ∼3690 cm^{-1} due to free O−H stretches is also observed, which can find its origin in both non-hydrogen-bonded water and Al−OH groups.[66] Interestingly, the shapes of the vSFG spectra at pH 4 (positively charged interface) and at pH 6 (net neutral charge) are similar, which suggests that the interfacial water molecules are aligned with their dipoles pointing away from the alumina surface, even at a net neutral surface. This is expected as most of the alumina surface is covered with Al_2−OH groups (∼15 OH group/nm^2)[67−70] and the interfacial water is aligned such that the oxygen atom is pointing to and the hydrogen atoms pointing away from the surface. The large difference in vSFG signal amplitude between pH 4 and pH 6 is because when the alumina surface is charged at pH 4, an electric field is generated at the alumina surface that extends into the bulk water and can orient water molecules via field−dipole interactions, resulting in an increase of the vSFG signal.

3.1.2. Halide Anion Effect on Water Ordering at Positively Charged α-Al_2O_3(0001)/H_2O Interface. Next to a positively charged alumina surface, the halide anions should behave as counterions and are expected to be closer to the interface than the cation (Na^+). The counterions next to a charged surface can screen the electrostatic surface charge and attenuate the vSFG

DOI: 10.1021/acs.jpcc.8b03004
J. Phys. Chem. C 2018, 122, 12819−12830

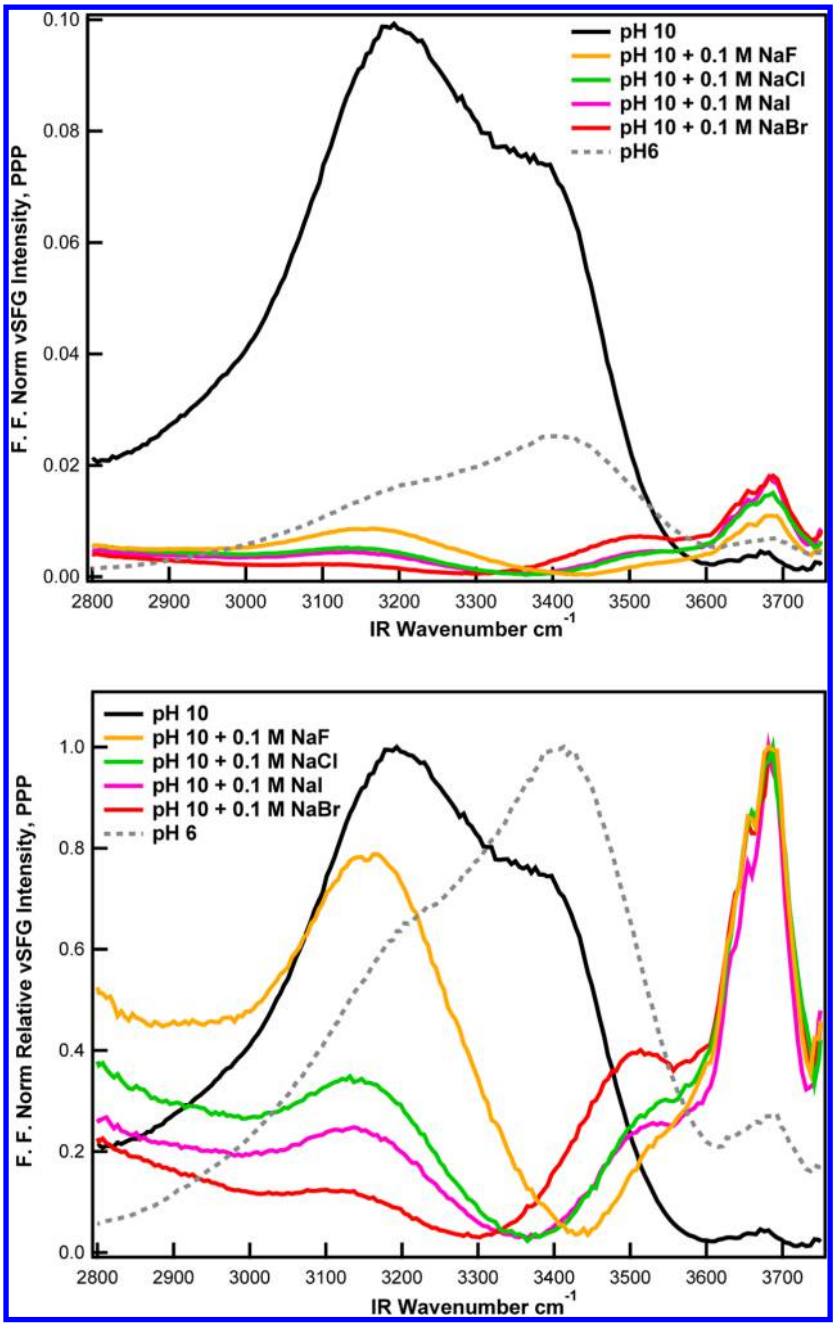

Figure 2. Effect of halide salts on the PPP-vSFG spectra of the α-$Al_2O_3(0001)/H_2O$ (pH 10) interface. The gray dotted line represents the vSFG spectra at pH 6, which is the PZC, i.e., net neutral surface charge. The colored solid lines represents the vSFG spectra at pH 4, where the surface is negatively charged without excess salt (black) and with 0.1 M NaF (yellow), NaCl (green), NaBr (red), and NaI (pink). The top figure compares the absolute intensity of different solutions, whereas the bottom figure has been normalized to the maximum peak to compare the relative intensities of different peaks. All data have been normalized with respect to the IR pulse profile and corrected for the wavelength dependence of the Fresnel factors, as described elsewhere.[11,12,72]

signal.[45,57,71] Hence, the halide anion with highest affinity to the interface should cause the most screening and result in the lowest vSFG signal. The halide salts (NaF, NaCl, NaBr, and NaI) attenuate the vSFG signal (Figure 1) in the order $F^- \gg Br^- > Cl^- > I^-$. This order is not affected by the sequence in which the halide salts are added (Figure S2-2, SI). Laser drift during the experiment as well as any possible surface dissolution had little to no effect on the vSFG signal, as evidenced from the quantitatively similar pH 6 spectra measured at the start, middle, and end of the experiments (Figure S2-1).

It is well known from the literature that small anions, e.g., F^-, interact more favorably with hydrophilic surfaces than bigger anions, e.g., I^-.[28−31] Since F^- has greater affinity for alumina surfaces, it should be the most effective at screening the positive surface charge. In contrast, larger anions like I^- are less attracted to the alumina surface and so should be the least effective at screening the positive surface charge. As a result, in the presence of F^-, the vSFG signal should have the least contribution from surface charge-oriented water molecules. Whereas, in the presence of I^-, lesser screening means there are more surface charge-oriented waters that contribute to the

DOI: 10.1021/acs.jpcc.8b03004
J. Phys. Chem. C 2018, 122, 12819−12830

vSFG signal. The effect of halide anions on the vSFG attenuation ($F^- \gg Br^- > Cl^- > I^-$) does not entirely follow the direct Hofmeister series and hence reflects the inconsistencies of relative anion affinity toward the alumina surface, as shown by previous studies.[14,15,17−21,25,26] Here, it is important to note that in the vSFG experiments, we are not directly measuring the anion affinity to alumina surface but inferring the relative anion affinity from the amount of ordered water remaining at the positively charged alumina surface in the presence of different anions.

3.1.3. Are Halide Anions Only Screening the Positive Surface Charge? An interesting observation is the large attenuation (20 times) of the vSFG signal in the presence of F^- in contrast to 2−3 times attenuation of the vSFG signal in the presence of other ions. In fact, the vSFG intensity in the presence of F^- ions is even lower than at pH 6 (Figure 1 top), which likely means that F^- has not only completely screened the positive surface charge but also possibly disrupted the interfacial water environment by displacing the interfacial water molecules due to contact adsorption of F^-. Recent Richmond et al.[37] and Tahara et al.[52] studies of anion effects on the interfacial water structure showed that if ions adsorb onto the interface and alter the interfacial hydrogen bonding environment, it causes a spectral shift of the O−H stretch or an overall change in the O−H stretch spectra. On the other hand, if the ions have lesser affinity to the interface, they should primarily shield the electrostatic surface charge with very little to no change in the interfacial hydrogen bonding environment, resulting in a uniform decrease of the spectral intensity (no spectral shift or change in the spectral shape).[37,52]

To compare the spectral shape, the vSFG spectra were normalized to the maximum peak (Figure 1 bottom). Upon addition of nonfluoride halide salts (NaCl, NaBr, and NaI), the intensity of the 3200 cm^{-1} peak is slightly reduced relative to the 3400 cm^{-1} peak, which points to a somewhat weaker hydrogen bonding environment. This is consistent with bulk studies where the O−H stretch of bulk water was observed to blue-shift upon addition of Cl^-, Br^- and I^- ions since the hydrogen bonding interaction between O−H and Cl^-, Br^-, or I^- is weaker than the hydrogen bonding interaction between O−H and O (in neat water).[54,73] In contrast, upon addition of NaF, along with the reduction of the 3200 cm^{-1} peak we also observe a slight red-shift of the 3200 cm^{-1} peak (Figure 1 bottom). This is also consistent with bulk studies that interpreted the red-shift to be due to strong hydrogen bonding interactions between the O−H and F^-.[54,73] However, apart from significant differences in attenuation of the vSFG signal, no large differences in the spectral shape in the vSFG signal were observed.

Our spectroscopic results are consistent with the notion that nonfluoride anions (Cl^-, Br^-, and I^-) are predominantly less attracted to the alumina surface and therefore do not undergo contact adsorption. These ions are mainly responsible for screening the surface charge, with only small perturbations in the interfacial hydrogen bonding environment. In contrast, the large attenuation of the vSFG signal in the presence of NaF salt could be evidence for F^- undergoing contact adsorption onto the alumina surface and in the process displacing the interfacial water molecules originally bound to the mineral surface. Therefore, at the positively charged $Al_2O_3(0001)/H_2O$ interface, F^- completely screens the surface charge and also changes the interfacial hydrogen bonding environment. A similar specific anion effect has been observed previously at the CaF_2/H_2O interface.[37]

3.2. Steady-State vSFG Study of Negatively Charged α-$Al_2O_3(0001)/H_2O$ Interfaces (pH 10). *3.2.1. Surface Charging of Negatively Charged α-$Al_2O_3(0001)/H_2O$ Interfaces.* The Al_2−OH functional groups undergo a deprotonation reaction in basic solution to form Al_2−O^-.[62] The vSFG signal for the negative surface (pH 10) is 3 times lower than for the positive surface (pH 4) at constant ionic strength, which is consistent with a previous vSFG study.[74] This difference in vSFG amplitude is consistent with the assignment of 3200 and 3400 cm^{-1} peaks originating mainly from the O−H stretches of interfacial water and surface aluminol groups, respectively. At a positively charged (pH 4) alumina surface, water molecules are expected to be oriented with their oxygen atom pointing to the surface (hydrogen down or H-down orientation) and hydrogen atom pointing away from the surface, which is similar to the dipole of the −OH groups from surface aluminol. As a result, both 3200 cm^{-1} (water) and 3400 cm^{-1} (aluminol) peaks have the same phase and constructively interfere to give rise to a large vSFG signal. In contrast, at a negatively charged surface, water is arranged with the hydrogen atoms pointing to the surface (hydrogen up or H-up orientation) and oxygen atoms pointing away from the surface. Therefore, the dipole of the O−H stretch of water is opposite to the dipole of the O−H stretch of the surface aluminol groups. Consequently, 3200 cm^{-1} (water) and 3400 cm^{-1} (aluminol) species destructively interfere, giving rise to a smaller vSFG signal at negative alumina surface (pH 10). This phase relationship between the 3200 and 3400 cm^{-1} peaks at the alumina (0001)/water interface was previously[41] demonstrated by the Shen group using heterodyne-detected vSFG measurements.

The vSFG spectral shape is also different for the positively (Figure 1) and negatively charged alumina/water interfaces (Figure 2). For the negatively charged alumina surface (pH 10), the 3200 cm^{-1} peak is larger than the 3400 cm^{-1} peak (Figure 2), whereas the opposite was true for the positively charged and neutral surfaces (Figure 1), which is consistent with previous vSFG studies[41,74] of alumina/water interfaces. This difference in shape of the vSFG spectra also supports the assignment of aluminol groups as mainly contributing to the 3400 cm^{-1} peak since at higher pH, the aluminol groups undergo deprotonation reaction, which reduces the number of O−H stretching vibrations from aluminol groups and hence the amplitude of the 3400 cm^{-1} peak. Alternatively, the difference in the vSFG spectral shape at positive and negative alumina surfaces could be related to the interfacial hydrogen bonding environment. Previous studies[75,76] have proposed that the strength of the hydrogen bonding environment of water can be examined by comparing the ratio of the 3200 and the 3400 cm^{-1} peaks. A ratio greater than 1 is an indication of water molecules in a strong hydrogen bonding environment and vice versa.[75,76] For the negative alumina surface, this ratio is ∼1.3, whereas for the positive alumina surface, the ratio is ∼0.6 (Figures 1 and 2). This could mean that the interfacial water next to a negatively charged surface is more strongly hydrogen bonded compared with the positively charged surface. This interpretation is in agreement with a recent theoretical study[77] that showed that the hydrogen bond donor water molecules (H-up) form stronger hydrogen bonds with the alumina surface compared with the hydrogen bond acceptor water molecules (H-down). On the other hand, the difference in the spectral shape for the positively and negatively charged alumina/water interface can

DOI: 10.1021/acs.jpcc.8b03004
J. Phys. Chem. C 2018, 122, 12819−12830

also be explained by considering the effect of the surface electric field on adjacent water molecules.[78] In that study, the perturbation of the O−H stretching frequency in the presence of anions was shown to be a direct result of the electric fields exerted by the anions on the adjacent hydrogen atoms of water molecules.[78] In contrast, the smaller effect of cations on the O−H stretching frequency was explained to be due to the hydrogen atom not being affected by the cation electric field since the OH bonds are oriented away from the point charge.[78] Similarly, in the case of negative alumina surfaces, hydrogen atoms are closer toward the negative surface charge, resulting in the vSFG spectra being enhanced in the 3200 cm^{-1} region. In contrast, hydrogen atoms point away from a positively charged alumina surface and electric field-induced effects on the O−H stretching frequency are absent. We recognize that all of these interpretations hinge on the assumption that the spectral shifts seen in the $|\chi^{(2)}|^2$ spectra obtained from the homodyne-detected vSFG experiments (such as in this study) are free from spectral deformation that could arise due to convolution between the real and the imaginary part of the $|\chi^{(2)}|^2$ spectra. However, Tahara et. al.[79] showed that this was not the case for homodyne-detected vSFG spectra and proposed that only the imaginary $\chi^{(2)}$ spectra obtained from heterodyne-detected vSFG measurements can be reliably compared. As a result, heterodyne-detected vSFG measurements may be required to further investigate this effect.

3.2.2. Halide Anion Effect on Water Ordering at Negatively Charged α-Al_2O_3(0001)/H_2O Interfaces. The addition of all halide salts significantly reduces the vSFG signal (Figure 2) to levels even lower than the signal for the neutral surface (pH 6). At the negatively charged alumina surface, cations are the counterions and are expected to be closest to the interface. The cations screen the negative surface charge and reduce the contribution from the water molecules oriented by the negative surface. Since Na^+ is the common cation for all the halide salts used in this study, a large reduction in the vSFG signal is observed for all halide salts. However, the reason why Na^+ (and other monovalent cations like K^+ and Cs^+, data not shown) causes a larger attenuation at a negative alumina surface compared with the positive alumina surface is not clear. Nevertheless, it is important to note that the pH at which salt attenuates the vSFG signal the largest is slightly above the PZC (pH 6−8) of the alumina surface. This is consistent with previous studies[1,2] on the salt effect at the silica/water interface, where the largest salt effect was also observed at pH 6−8, which is greater than the PZC of silica (pH 2). Interestingly, two oppositely pointing O−H stretching vibrations were also observed at pH 7 for silica/water interface.[64] Therefore, we speculate that the pH at which ions largely attenuate the vSFG signal could be correlated to the presence of oppositely oriented O−H stretching modes. This observation definitely deserves future theoretical and experimental investigations.

Even though the halide anions are expected to be repelled from the negative alumina surface, anion specificity is still observed, as evidenced by the differences in the attenuated vSFG signals. Since the vSFG signal is sensitive to the identity of the anion, it is very likely that the cation (Na^+) and the anions (F^-, Cl^-, Br^-, and I^-) adsorb onto the negatively charged alumina surface as ion pairs. The attenuated vSFG signal follows the sequence $Br^- > I^- \approx Cl^- > F^-$, which is in partial agreement with the indirect Hofmeister ranking (I^- being the exception). This order is not affected by the sequence in which the halide salts are added (Figure S2-3, SI). The vSFG signal in the presence of I^- and Cl^- are very close to each other and sometimes interchanged (Figure S2-3, SI). However, inferring the anion affinity to the negatively charged alumina surface from the degree of the vSFG signal attenuation is not straightforward since halide anions are not the counterions (Na^+ is the counterion).

The observed trend of vSFG signal attenuation can be explained in two ways: (1) Larger anions, e.g., Br^-, have greater affinity for the negative alumina surface compared with F^-, and therefore the Na^+−Br^- ion pairs are more effective at screening the negative surface charge compared to the Na^+−F^- ion pair. Consequently, the vSFG signal in the presence of NaBr is lower than NaF. (2) Small anions such as F^- have a higher affinity toward alumina, and therefore the presence of F^- adds to the negative charge at the interface, resulting in the largest vSFG signal at pH 10. In contrast, larger anions (Br^- and I^-) have lower affinity for the hydrophilic alumina surface and therefore are not able to increase the negative charge at the interface; resulting in the lowest vSFG signal at pH 10. However, since vSFG experiments do not directly measure the ion affinity of a surface, it is not possible to know which anion has greater affinity toward the negatively charged alumina surface. Given that most previous studies[14,15,17,18,20] have reported smaller anions, e.g., F^-, having a greater affinity to alumina surfaces (surface charge was not reported in these studies) compared with larger anions, e.g., Br^-, the second explanation is more likely. Theoretical studies on surface charge-dependent ion adsorption could be helpful in answering these questions.

3.2.3. Halide Salt Changes the Water Structure Next to Negative Alumina Surfaces. Halide salts next to the negatively charged alumina surface (pH 10) also change the shape of the vSFG spectra (Figure 2 bottom). In the absence of salt, two major peaks at ∼3200 and 3400 cm^{-1} are present. Upon addition of salt, only one major peak at ∼3150 cm^{-1} is observed and a minimum is observed near ∼3400 cm^{-1}. A side peak at 3500 cm^{-1} is also observed whose ion specificity sequence is reversed compared to that of the 3200 cm^{-1} peak. Interestingly, a point of inflection is observed at ∼3300 cm^{-1} region, which possibly indicates the presence of opposite pointing O−H stretching vibrations at the interface, which is also consistent with the phase relationship between 3200 and 3400 cm^{-1} peaks next to the negatively charged alumina/water interface discussed earlier. The disappearance of the 3400 cm^{-1} peak in the presence of halide salts is speculated to be due to deprotonation of aluminol groups and/or simply due to destructive interference between oppositely pointing O−H stretching dipoles. The large attenuation of the vSFG signal and the change in the spectral shape upon addition of halide salts is likely an indication of ions altering the interfacial water arrangement. Additionally, a large intensity in the lower frequency region (<2900 cm^{-1}) is also observed, which we have assigned previously to strongly hydrogen-bonded surface aluminol groups and/or interfacial water molecules forming strong hydrogen bonds to the surface.[11,12] This low-frequency mode is also present at the positively charged alumina/water interfaces but is overshadowed by the large signal due to 3200 and 3400 cm^{-1} species.

3.3. Time-Resolved vSFG Study of α-Al_2O_3(0001)/H_2O Interface. The steady-state vSFG spectra discussed above show that the effect of ions on the structure of water next to a charged alumina surface partially correlates with the direct and indirect Hofmeister series, depending on the sign of the surface charge. The next step is to investigate whether the presence of

DOI: 10.1021/acs.jpcc.8b03004
J. Phys. Chem. C 2018, 122, 12819−12830

halide salts at the alumina/water interface can disrupt the vibrational dynamics of interfacial water. Therefore, we employed time-resolved vSFG (IR pump-integrated vSFG probe) to measure the vibrational relaxation dynamics of the interfacial O−H stretch to better understand the influence of halide ions next to the positively (Figure 3) and negatively (Figures 4 and 5) charged alumina/water interfaces.

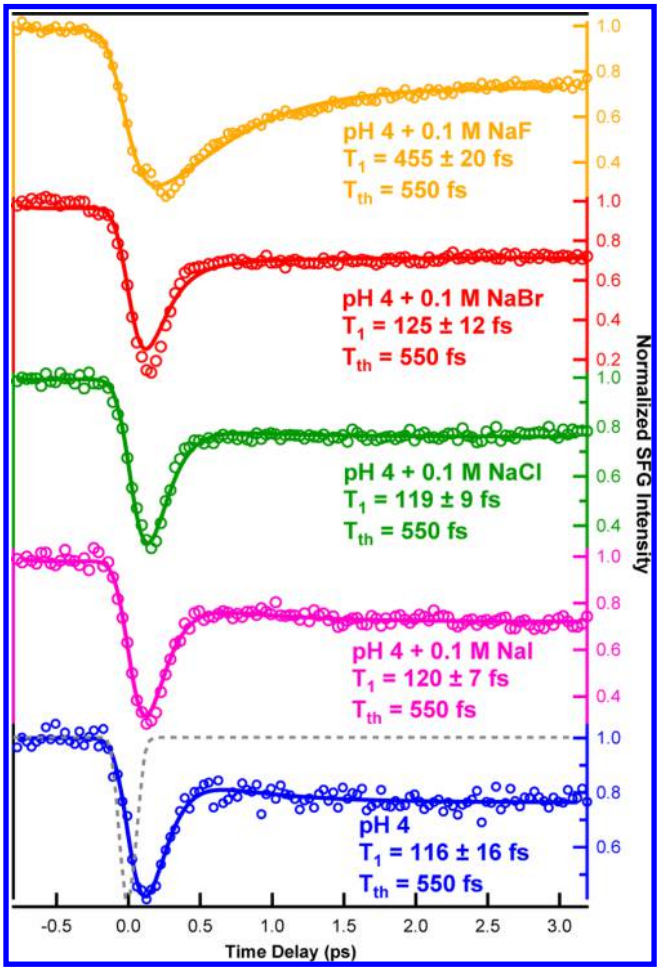

Figure 3. IR pump-integrated vSFG probe vibrational dynamics of the interfacial OH species at the α-$Al_2O_3(0001)/H_2O$ interface for bulk pH 4 without excess salt (blue) and with 0.1 M NaF (yellow), NaCl (green), NaBr (red), and NaI (pink). The solid lines are the best fits with a four-level system, which have been described elsewhere[11,12] and in Section 3 of the SI. Details of fitting are discussed in Section 3 of the SI. The instrument response function (IRF) is shown by the gray dashed line. P-polarized IR pump and PPP-polarized vSFG probe were used.

The vibrational dynamics of the O−H stretch is known to be a sensitive probe of its hydrogen bonding environment and has been used to investigate the effect of ions on hydrogen bonding strength in both bulk[53,54,73,80] and interfacial water.[11,12,52,57] The models used to fit the time-resolved vSFG data and its limitations are described in Section 3 of the SI. However, since we are pumping and probing from the 2850−3200 cm^{-1} region, which includes two types of O−H stretches (~3200 and ~2900 cm^{-1}), the validity of these models is also briefly discussed while analyzing the IR pump spectrally resolved vSFG probe data. Typically, the kinetics for an excited O−H stretch mode to relax back to its ground state is modeled by a four-level

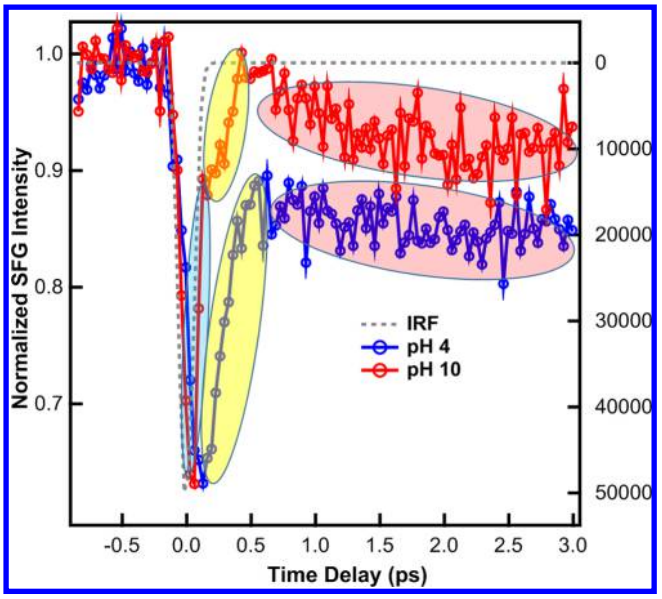

Figure 4. IR pump-integrated vSFG probe vibrational dynamics of the interfacial OH species at the α-$Al_2O_3(0001)/H_2O$ interface for bulk pH 4 (blue) and bulk pH 10 (red) without excess salt. The blue, yellow, and red ellipses represent the T_0, T_1, and T_{th} time scales, respectively, described in the text. The IRF is shown by the gray dashed line. P-polarized IR pump and PPP-polarized vSFG probe were used.

model consisting of two time scales: vibrational lifetime (T_1) and thermalization (T_{th}).[11,12,55,56,81] T_1 represents the time taken for an O−H stretch mode to relax from the first excited state (ν = 1) to an intermediate state ($\nu = \nu^*$), which is generally accepted to be the overtone of the water bending mode.[57,82,83] T_{th} represents the time taken for the intermediate state ($\nu = \nu^*$) to relax a hot quasiequilibrium ground state (ν = 0*). The T_1 of an O−H stretch mode is directly affected by its hydrogen bonding environment (i.e., shorter vibrational lifetime is an indication of strong hydrogen bonds and/or increase in the number of hydrogen bonding partners). The T_1 values obtained from fitting the time-resolved measurements in this study represent the apparent lifetime of the excited O−H stretch due to the limitation of the experiment, as discussed in Section 3 of the SI.

3.3.1. Halide Anion Effect on Vibrational Dynamics at Positively Charged α-$Al_2O_3(0001)/H_2O$ Interfaces. At the positively charged alumina surface (pH 4) in the absence of excess salts, the vibrational lifetime of the interfacial O−H stretch (T_1 ~ 116 fs) is shorter than that of bulk water (T_1 = 190−260 fs),[53,84−86] consistent with our previous study.[12] It is clear that the vibrational relaxation at pH 4 is not limited by the instrument response function (IRF), which is measured by recording the third-order cross-correlation between IR pump, IR probe, and visible beam (Figure 3). The definition of time zero (in Figures 3−5) is described in Section 4 of the SI. Addition of excess halide ions (0.1 M NaCl, NaBr, and NaI), does not affect the T_1 lifetime (Figures 3, S5-1, SI, and Table 1). This is consistent with our previous interpretation of the spectroscopic result (Figure 1) which suggested that the nonfluoride anions (Cl^-, Br^-, and I^-) have lesser affinity for the alumina surface (no contact adsorption) and were mainly responsible for screening the surface charge, with only small perturbations in the interfacial hydrogen bonding environment. In contrast, when NaF was added to the positively charged

DOI: 10.1021/acs.jpcc.8b03004
J. Phys. Chem. C 2018, 122, 12819−12830

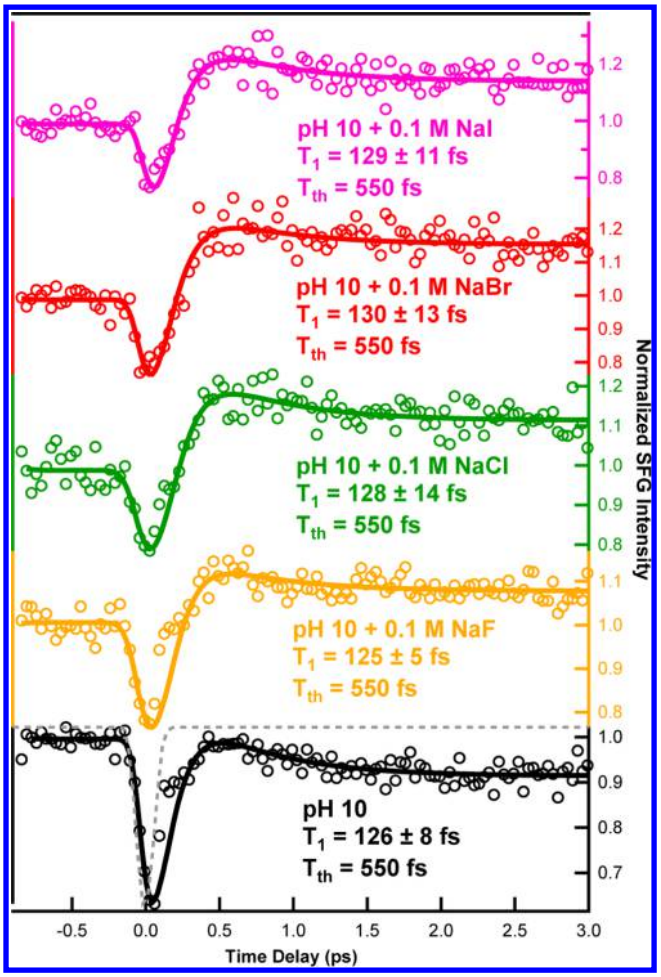

Figure 5. IR pump-integrated vSFG probe vibrational dynamics of the interfacial OH species at the α-Al_2O_3(0001)/H_2O interface for bulk pH 10 without excess salt (black) and with 0.1 M NaF (yellow), NaCl (green), NaBr (red), and NaI (pink). The solid lines are the best fits with a four-level system (excluding the T_0 component), which have been described elsewhere[11,12] and in Section 3 of the SI. Details of fitting the pH 10 data are discussed in Section 3 of the SI. The IRF is shown by the gray dashed line; P-polarized IR pump and PPP-polarized vSFG probe were used.

alumina/water interface, the vibrational relaxation slowed down by 4 times (T_1 = 455 fs). This is also consistent with our previous interpretation of the spectroscopic result (Figure 1) where we suggested that that F^- alters the interfacial hydrogen bonding environment by undergoing contact adsorption and hence changing the structure and bonding (chemistry) of water at the alumina surface.

As previously discussed, F^- caused a slight red-shift in the O−H stretch frequency, which usually means stronger hydrogen bonding and this should lead to a shorter vibrational lifetime. Bulk studies have shown that the water molecules forming the solvation shell of F^- show short vibrational lifetimes, similar to bulk water.[54] Therefore, it is surprising that the vibrational dynamics at the positively charged alumina surface slowed down by 4 times in the presence of F^- counterions. This suggests that the slowing down of vibrational relaxation upon addition of NaF is not due to probing of water molecules solvating F^-. However, a complete understanding of the role of F^- in changing the interfacial water arrangement in such a way that it lengthens the interfacial vibrational lifetime is not clear from the IR pump-integrated vSFG probe measurements alone.

To better understand the effect of F^- on the vibrational dynamics of water next to positively charged alumina (0001) surfaces, IR pump spectrally resolved vSFG probe data (Figure S7-1, SI) were also collected. Before the arrival of the pump IR beam, the spectrally resolved data is featureless. When the pump IR is temporally overlapped with the vSFG probe, three significant features are observed close to time zero:

(a) A bleach (decreased vSFG signal) is observed around 3200 cm^{-1}, which can be assigned to $\nu = 1 \leftarrow 0$ transition, which was clearly observed in the vSFG spectra of the alumina/water interface (Figure 1).

(b) An increase in vSFG signal is observed at around 2900 cm^{-1}, which could be due to a hot band ($\nu = 2 \leftarrow 1$) transition of the 3200 cm^{-1} species. This suggests an anharmonicity of ~300 cm^{-1}, which is consistent with the bulk water value.[52,85,87] This increase in vSFG signal could also be due to the coherent artifact. Although the large intensity of this feature supports the coherent artifact assignment, the wavelength dependence nature does not. Since this feature is present near the edge of the IR profile, its nature and dynamics are not clear from the experiments. The presence of this feature calls into question the validity of the four-level model used to fit the IR pump-integrated vSFG probe data discussed earlier, which does not account for any mechanism responsible for increase in vSFG signal near time zero. However, the increase in vSFG signal is limited in the low-frequency region and should only have minimal effect on the T_1 lifetime extracted using the four-level model.

(c) A bleach is also observed around 2900 cm^{-1} right after the increased vSFG signal, which is due to $\nu = 1 \leftarrow 0$ transition of the low-frequency species (<2900 cm^{-1}) at the alumina/water interface. As previously stated, this feature has only been recently assigned and the observation of a bleach in the IR pump spectrally resolved vSFG probe data confirms its existence at the alumina (0001)/water interface.

The IR pump spectrally resolved vSFG probe data also shows that the halide salts (0.1 M NaCl, NaBr, and NaI) do not affect the dynamics of any of the three features discussed above (Figure S7-1, SI). Hence, the T_1 lifetime remains unaltered in the IR pump- integrated vSFG probe measurements discussed earlier. However, upon addition of 0.1 M NaF, we can clearly

Table 1. T_1 Obtained from Fitting the IR Pump-Integrated vSFG Probe Data Using the Four Level Model[a]

	no salt	NaF	NaCl	NaBr	NaI
pH 4	116 ± 16	455 ± 20	119 ± 9	125 ± 12	120 ± 7
pH 10	126 ± 8	125 ± 5	128 ± 14	130 ± 13	129 ± 11

[a]The error bars are the standard deviation of the results of 3−4 independent experiments. The details of the four level model and the fitting procedure are described in Section 3 of the SI. T_{th} was fixed at 550 fs in all cases.

DOI: 10.1021/acs.jpcc.8b03004
J. Phys. Chem. C 2018, 122, 12819−12830

observe that the bleach around 2900 cm^{-1} lasts much longer whereas the bleach around 3200 cm^{-1} is only slightly affected.

To clearly see this effect, the spectrally resolved data is separated into two regions of interest by integrating the SFG signal >3000 and <3000 cm^{-1} (Figure S7-2, SI). For the >3000 cm^{-1} region, it is clear that the presence of NaCl does not affect the vibrational dynamics next to the positively charged alumina/water interface. However, in the presence of NaF, the vibrational dynamics can be seen to slow down due to the slow decaying component at t > 300 fs. For the <3000 cm^{-1} region, the kinetics of vibrational relaxation is dominated by an induced absorption at t < 0 ps, followed by a bleach at t > 0 ps, which recovers rapidly in the absence of excess salts. In the presence of nonfluoride salts (NaCl, NaBr, and NaI), the recovery of bleach is similar to that in the no salt case. However, when NaF is present, the bleach recovery is very slow. From these results, we hypothesize that F^- ions mainly affects the vibrational dynamics of strongly hydrogen bonded O−H groups (<3000 cm^{-1} species).

To further confirm this, the IR pump and probe window was slightly blue-shifted (Figure S8-1, SI) to 3000−3300 cm^{-1} (instead of 2800−3100 cm^{-1} region) and the integrated time-resolved vSFG measurements were repeated (Figure S8-2, SI). The vibrational dynamics of pH 4 and pH 4 + 0.1 M NaCl are identical. However, addition of 0.1 M NaF introduces a slowly decaying component but its contribution to the overall vibrational dynamics is now much smaller. This further strengthens our argument that F^- mainly interacts with the <3000 cm^{-1} O−H species at the positively charged alumina/water interface and, slows down the vibrational dynamics of water.

It is well known that F^- tends to remain hydrated.[88−90] So when F^- approaches the positively charged alumina/water interface, it could break the strong hydrogen bonding interaction so that the F^- forms its hydration shell with the surrounding water molecules and the surface aluminol groups. As a result, a pathway for fast energy transfer between the water molecules and the surface aluminol groups is absent. This would lead to a slowing down of vibrational lifetime of the <2900 cm^{-1} species. Additionally, F^- is known to have a strong affinity to protons. If the interfacial protons are bound to the F^-, this could also slow down the vibrational relaxation since proton transfer is speculated to be an important mechanism of vibrational relaxation at the alumina/water interface.[12]

Lastly, at a positively charged surface, irrespective of whether halide salts are present or not, the decreased vSFG signal does not recover to the initial value (level before pump IR arrives) on the time scale of the experiment (Figure 3). This is an indication that the IR pump has increased the local temperature of the water and as a result has weakened the hydrogen bonds of water, which has been observed previously as a blueshift of the vSFG spectra.[52,55,91]

3.3.2. Halide Anion Effect on Vibrational Dynamics at Negatively Charged α-Al_2O_3(0001)/H_2O Interfaces. The vibrational dynamics of water next to a negatively charged alumina surface is different from that next to the positively charged alumina surface (Figure 4), which clearly shows three different time scales: the fast IRF limited time scale (T_0, shaded blue), T_1 time scale (shaded red), and T_{th} time scale (shaded yellow). As a result, the data for pH 10 data cannot be entirely fit with the four-level model. This is in contrast to our previous study[12] at the negatively charged Al_2O_3(0001)/H_2O interface where the vibrational dynamics was slower than the IRF and was successfully fit using the four-level model. The difference could stem from the use of a lower frequency IR pump−probe window in the current study compared to the previous study.

The origin of the T_0 component for negatively charged alumina is not clear, but it cannot be due to the coherent artifact since coherent artifacts are typically not sensitive to solution pH or ion identity (the T_0 component is absent for positively charged alumina surfaces, and the T_0 amplitude is affected by anion identity at negative alumina surfaces). To fit the pH 10 data with the four-level model, the initial fast T_0 component is neglected by rejecting the first 100 fs data points after the maximum bleach during the fitting procedure, as described in Section 3 of the SI. The T_1 and T_{th} time scales are sufficient to accurately explain the majority of pH 10 data (Figure 5 and Table 1).

The halide salts (0.1 M NaF, NaCl, NaBr, and NaI) affect the vibrational dynamics at the negatively charged Al_2O_3(0001)/H_2O interface (Figures 5 and S6-1, SI) in two ways. First, the amplitude of the T_0 component is reduced in the sequence NaBr > NaI > NaCl > NaF (Figure S6-1, SI), which is identical to the sequence of the attenuated vSFG signal (Figure 2). As the origin of the T_0 component is unclear, the significance of trends associated with amplitude variations in the presence of different halide salts is also unknown. Second, in the presence of the halide salts, the vSFG signal recovers beyond the initial value after the bleach, suggesting that the IR pump causes an increase in the population of the strongly hydrogen bonded O−H species. Such behavior has been previously observed only when pumping and probing the weakly hydrogen bonded O−H species.[56] The bleach recovery beyond the initial value in the presence of halide salts while pumping and probing the strongly hydrogen bonded region could be related to the presence of unique arrangements of water molecules (opposite pointing water species dipole, as discussed earlier) at the negatively charged alumina surface in the presence of ions. However, it is not possible to definitively ascertain the origin of this behavior from our data.

It is clear from the fit results (Table 1) that although the presence of halide salts affects the vibrational relaxation at the negatively charged alumina/water interface by reducing the amplitude of the T_0 component (Figure S6-1, SI), T_1 remains, more or less, unaffected. This result is surprising since when NaF salt largely attenuated the vSFG signal at the positively charged alumina/water interface, T_1 slowed down by 4 times, as discussed earlier. Therefore, since all the halide salts largely attenuated the vSFG signal and also altered the vSFG spectral shape at negatively charged alumina/water interfaces (Figure 2), we expected T_1 to also slow down for all the halide salts. However, the invariable T_1 of the negatively charged alumina/water interface in the presence of halide salts suggests that there is no obvious correlation between attenuation of the vSFG signal and T_1.

The reason for NaF slowing down the vibrational dynamics at the positively charged alumina surface but not at the negatively charged alumina surface is surprising. This can be explained if we take the identity of the counterion into consideration. At a positively charged surface, the main counterion is F^-, which breaks the strong hydrogen bonding interaction between the interfacial water molecules and the surface aluminol groups and causes the large vSFG attenuation and the vibrational relaxation of interfacial water to slow down. In contrast, at a negatively charged surface, Na^+ is the main counterion and although it is effective at screening the negative

DOI: 10.1021/acs.jpcc.8b03004
J. Phys. Chem. C 2018, 122, 12819−12830

surface charge (large attenuation of vSFG signal) and also perturbing the interfacial hydrogen bonding environment (change in vSFG spectral shape), Na^+ counterions are not able to break the strong interaction between the surface and the water molecules and hence the vibrational lifetime remains unchanged. Additionally, it is well known that the cation effect on the properties of bulk water is less than the anion effect.[53,73] However, whether this effect extends to the interface is not known and our data while suggestive are not sufficient to answer this question.

To further examine the interaction between halide salts and the negatively charged alumina/water interface, IR pump spectrally resolved vSFG probe measurements were acquired (Figure S7-1, SI). Similar to the positive alumina/water interface, the negative alumina/water interface also shows three significant features (bleach of 3200 cm^{-1} species, hot band, and the bleach of the 2900 cm^{-1} species) around time zero. None of the halide salts (NaF, NaCl, NaBr, and NaI) slow down the vibrational dynamics, which confirms our hypothesis that the type of interaction observed between F^- and the strongly hydrogen-bonded O−H species at the positively charged alumina/water interface is absent at the negatively charged alumina/water interface. We avoid doing further analysis and fitting our spectrally resolved data because our one color pump probe experimental limitation does not capture the entire O−H stretching region (2800−3800 cm^{-1}), which is probably highly coupled. Therefore, any sophisticated analysis on the limited bandwidth spectrally resolved data presented here would be inconclusive.

4. CONCLUSIONS

Steady-state and time-resolved vibrational sum frequency generation (vSFG) spectroscopy were used to investigate the effects of halide salts on the interfacial hydrogen bonding environment next to charged $Al_2O_3(0001)$ surfaces. Halide ions shielded the positively charged alumina and attenuated the vSFG signal in the sequence $F^- \gg Br^- > Cl^- > I^-$. In contrast, the countercation Na^+ was mainly responsible for shielding the negatively charged alumina/water interface. Anion specificity is still observed at negatively charged alumina surfaces, as revealed by the sequence of the attenuated vSFG signal ($Br^- > I^- \approx Cl^- > F^-$). Hence, the effect of halide ions on the SFG signal next to positively and negatively charged alumina surfaces followed direct and indirect Hofmeister series (with minor exceptions), respectively. The vibrational dynamics of water next to positively charged alumina surfaces was fast (T_1 = 116 fs) and only slowed down (T_1 = 455 fs) in the presence of F^-. IR pump spectrally resolved vSFG probe experiments revealed that F^- decelerated vibrational relaxation by possibly weakening the hydrogen bonding interaction between the surface and the adjacent water molecules and/or by blocking the proton transfer pathway. In contrast, the vibrational dynamics of water next to the negatively charged alumina surface is different from that next to the positively charged alumina surface and the presence of halide salts affects the vibrational relaxation kinetics in a unique manner. Our results clearly show that the anion effect on the structure and dynamics of water next to alumina is surface charge dependent, which possibly explains the inconsistencies in the relative anion adsorption affinity for alumina surfaces reported in the literature.

■ ASSOCIATED CONTENT

Supporting Information

The Supporting Information is available free of charge on the ACS Publications website at DOI: 10.1021/acs.jpcc.8b03004.

Sample preparation and experimental setup for the steady-state and time-resolved vSFG measurements; VSFG reproducibility experiments model used for fitting the time-resolved vSFG data; definition of time zero in the time-resolved vSFG data; IR pump spectrally resolved vSFG probe vibrational dynamics of the interfacial OH species at the α-$Al_2O_3(0001)/H_2O$ interface for bulk pH 4 and pH 10 with/without salts 0.1 M NaI, NaCl, NaBr, and NaF; vibrational dynamics of α-$Al_2O_3(0001)/H_2O$ interface for bulk pH 4 with/without 0.1 M NaCl and NaF using a blue-shifted IR pump and vSFG probe (PDF)

■ AUTHOR INFORMATION

Corresponding Author

*E-mail: eborguet@temple.edu.

ORCID

Aashish Tuladhar: 0000-0003-2449-4984

Notes

The authors declare no competing financial interest.

■ ACKNOWLEDGMENTS

The authors acknowledge the National Science Foundation for supporting this work (NSF Grant CHE 1337880). The authors thank Professor M. Zdilla (Temple University, Chemistry Department) for alumina prism face orientation identification by X-ray diffraction and Dr. Kyle Gilroy (Professor S. Neretina Group, Temple University, College of Engineering) for gold coating of the alumina prisms. The authors thank Dr. Richard C. Remsing and Dr. Mark DelloStritto for helpful discussions.

■ REFERENCES

(1) Dove, P. M. The Dissolution Kinetics of Quartz in Sodium Chloride Solutions at 25 Degrees to 300 Degrees C. *Am. J. Sci.* **1994**, *294*, 665−712.

(2) Dewan, S.; Yeganeh, M. S.; Borguet, E. Experimental Correlation Between Interfacial Water Structure and Mineral Reactivity. *J. Phys. Chem. Lett.* **2013**, *4*, 1977−1982.

(3) Catalano, J. G. Weak Interfacial Water Ordering on Isostructural Hematite and Corundum (001) Surfaces. *Geochim. Cosmochim. Acta* **2011**, *75*, 2062−2071.

(4) Stumm, W. *Chemistry of the Solid-Water Interface: Processes at the Mineral-Water and Particle-Water Interface in Natural Systems*; John Wiley & Son Inc., 1992.

(5) Hass, K. C.; Schneider, W. F.; Curioni, A.; Andreoni, W. The Chemistry of Water on Alumina Surfaces: Reaction Dynamics from First Principles. *Science* **1998**, *282*, 265−268.

(6) Furlong, B. K.; Hightower, J. W.; Chan, T. Y.-L.; Sarkany, A.; Guczi, L. 1, 3-Butadiene Selective Hydrogenation over Pd/Alumina and CuPd/Alumina Catalysts. *Appl. Catal., A* **1994**, *117*, 41−51.

(7) Knözinger, H.; Ratnasamy, P. Catalytic Aluminas: Surface Models and Characterization of Surface Sites. *Catal. Rev.* **1978**, *17*, 31−70.

(8) Leenaars, A.; Keizer, K.; Burggraaf, A. The Preparation and Characterization of Alumina Membranes with Ultra-Fine Pores. *J. Mater. Sci.* **1984**, *19*, 1077−1088.

(9) Miesse, C. M.; Masel, R. I.; Jensen, C. D.; Shannon, M. A.; Short, M. Submillimeter-Scale Combustion. *AIChE J.* **2004**, *50*, 3206−3214.

(10) Ravishankar, N.; Shenoy, V. B.; Carter, C. B. Electric Field Singularity Assisted Nanopatterning. *Adv. Mater.* **2004**, *16*, 76−80.

(11) Tuladhar, A.; Dewan, S.; Kubicki, J. D.; Borguet, E. Spectroscopy and Ultrafast Vibrational Dynamics of Strongly Hydrogen Bonded OH Species at the α-Al_2O_3(11−20)/H_2O Interface. *J. Phys. Chem. C* **2016**, *120*, 16153−16161.
(12) Tuladhar, A.; Piontek, S. M.; Borguet, E. Insights on Interfacial Structure, Dynamics, and Proton Transfer from Ultrafast Vibrational Sum Frequency Generation Spectroscopy of the Alumina(0001)/Water Interface. *J. Phys. Chem. C* **2017**, *121*, 5168−5177.
(13) Tschapek, M.; Wasowski, C.; Sanchez, R. T. The PZC and IEP of γ-Al_2O_3 and TiO_2. *J. Electroanal. Chem. Interfacial Electrochem.* **1976**, *74*, 167−176.
(14) Lützenkirchen, J. Specific Ion Effects at Two Single-Crystal Planes of Sapphire. *Langmuir* **2013**, *29*, 7726−7734.
(15) Sprycha, R. Electrical Double Layer at Alumina/Electrolyte Interface: I. Surface Charge and Zeta Potential. *J. Colloid Interface Sci.* **1989**, *127*, 1−11.
(16) D'Aniello, M. J. Anion Adsorption on Alumina. *J. Catal.* **1981**, *69*, 9−17.
(17) Borah, J. M.; Mahiuddin, S.; Sarma, N.; Parsons, D. F.; Ninham, B. W. Specific Ion Effects on Adsorption at the Solid/Electrolyte Interface: A Probe into the Concentration Limit. *Langmuir* **2011**, *27*, 8710−8717.
(18) Das, M. R.; Borah, J. M.; Kunz, W.; Ninham, B. W.; Mahiuddin, S. Ion Specificity of the Zeta Potential of α-Alumina, and of the Adsorption of p-Hydroxybenzoate at the α-Alumina−Water Interface. *J. Colloid Interface Sci.* **2010**, *344*, 482−491.
(19) Johnson, S. B.; Scales, P. J.; Healy, T. W. The Binding of Monovalent Electrolyte Ions on α-Alumina. I. Electroacoustic Studies at High Electrolyte Concentrations. *Langmuir* **1999**, *15*, 2836−2843.
(20) Franks, G. V.; Johnson, S. B.; Scales, P. J.; Boger, D. V.; Healy, T. W. Ion-Specific Strength of Attractive Particle Networks. *Langmuir* **1999**, *15*, 4411−4420.
(21) Piasecki, W.; Zarzycki, P.; Charmas, R. Adsorption of Alkali Metal Cations and Halide Anions on Metal Oxides: Prediction of Hofmeister Series Using 1-pK Triple Layer Model. *Adsorption* **2010**, *16*, 295−303.
(22) Quezada, G. R.; Rozas, R. E.; Toledo, P. G. Molecular Dynamics Simulations of Quartz (101)-Water and Corundum (001)-Water Interfaces: Effect of Surface Charge and Ions on Cation Adsorption, Water Orientation, and Surface Charge Reversal. *J. Phys. Chem. C* **2017**, *121*, 25271−25282.
(23) Sverjensky, D. A.; Fukushi, K. Anion Adsorption on Oxide Surfaces: Inclusion of the Water Dipole in Modeling the Electrostatics of Ligand Exchange. *Environ. Sci. Technol.* **2006**, *40*, 263−271.
(24) Parsons, D. F.; Bostrom, M.; Maceina, T.; Salis, A.; Ninham, B. W. Why Direct or Reversed Hofmeister Series? Interplay of Hydration, Non-Electrostatic Potentials, and Ion Size. *Langmuir* **2010**, *26*, 3323−3328.
(25) Sahai, N. Estimating Adsorption Enthalpies and Affinity Sequences of Monovalent Electrolyte Ions on Oxide Surfaces in Aqueous Solution. *Geochim. Cosmochim. Acta* **2000**, *64*, 3629−3641.
(26) Sverjensky, D. A. Prediction of Surface Charge on Oxides in Salt Solutions: Revisions for 1: 1 (M^+L^-) Electrolytes. *Geochim. Cosmochim. Acta* **2005**, *69*, 225−257.
(27) Lyklema, J. Simple Hofmeister Series. *Chem. Phys. Lett.* **2009**, *467*, 217−222.
(28) Bastos-González, D.; Pérez-Fuentes, L.; Drummond, C.; Faraudo, J. Ions at Interfaces: the Central Role of Hydration and Hydrophobicity. *Curr. Opin. Colloid Interface Sci.* **2016**, *23*, 19−28.
(29) Schwierz, N.; Horinek, D.; Netz, R. R. Reversed Anionic Hofmeister Series: the Interplay of Surface Charge and Surface Polarity. *Langmuir* **2010**, *26*, 7370−7379.
(30) Schwierz, N.; Horinek, D.; Netz, R. R. Anionic and Cationic Hofmeister Effects on Hydrophobic and Hydrophilic Surfaces. *Langmuir* **2013**, *29*, 2602−2614.
(31) Schwierz, N.; Horinek, D.; Sivan, U.; Netz, R. R. Reversed Hofmeister Series—The Rule Rather Than the Exception. *Curr. Opin. Colloid Interface Sci.* **2016**, *23*, 10−18.
(32) Gurau, M. C.; Lim, S.-M.; Castellana, E. T.; Albertorio, F.; Kataoka, S.; Cremer, P. S. On the Mechanism of the Hofmeister Effect. *J. Am. Chem. Soc.* **2004**, *126*, 10522−10523.
(33) Chen, X.; Yang, T.; Kataoka, S.; Cremer, P. S. Specific Ion Effects on Interfacial Water Structure near Macromolecules. *J. Am. Chem. Soc.* **2007**, *129*, 12272−12279.
(34) Chen, X.; Flores, S. C.; Lim, S.-M.; Zhang, Y.; Yang, T.; Kherb, J.; Cremer, P. S. Specific Anion Effects on Water Structure Adjacent to Protein Monolayers. *Langmuir* **2010**, *26*, 16447−16454.
(35) Nihonyanagi, S.; Yamaguchi, S.; Tahara, T. Counterion Effect on Interfacial Water at Charged Interfaces and Its Relevance to the Hofmeister Series. *J. Am. Chem. Soc.* **2014**, *136*, 6155−6158.
(36) Flores, S. C.; Kherb, J.; Konelick, N.; Chen, X.; Cremer, P. S. The Effects of Hofmeister Cations at Negatively Charged Hydrophilic Surfaces. *J. Phys. Chem. C* **2012**, *116*, 5730−5734.
(37) Hopkins, A. J.; Schrödle, S.; Richmond, G. L. Specific Ion Effects of Salt Solutions at the CaF_2/Water Interface. *Langmuir* **2010**, *26*, 10784−10790.
(38) DeWalt-Kerian, E. L.; Kim, S.; Azam, M. S.; Zeng, H. B.; Liu, Q. X.; Gibbs, J. M. pH-Dependent Inversion of Hofmeister Trends in the Water Structure of the Electrical Double Layer. *J. Phys. Chem. Lett.* **2017**, *8*, 2855−2861.
(39) Sung, J.; Zhang, L.; Tian, C.; Shen, Y. R.; Waychunas, G. A. Effect of pH on the Water/α-Al_2O_3 (1102) Interface Structure Studied by Sum-Frequency Vibrational Spectroscopy. *J. Phys. Chem. C* **2011**, *115*, 13887−13893.
(40) Sung, J.; Shen, Y.; Waychunas, G. The Interfacial Structure of Water/Protonated α-Al_2O_3 (11-20) as a Function of pH. *J. Phys.: Condens. Matter* **2012**, *24*, No. 124101.
(41) Zhang, L.; Tian, C.; Waychunas, G. A.; Shen, Y. R. Structures and Charging of α-Alumina (0001)/Water Interfaces Studied by Sum-Frequency Vibrational Spectroscopy. *J. Am. Chem. Soc.* **2008**, *130*, 7686−7694.
(42) Becraft, K.; Richmond, G. In situ Vibrational Spectroscopic Studies of the CaF_2/H_2O Interface. *Langmuir* **2001**, *17*, 7721−7724.
(43) Hua, W.; Verreault, D.; Huang, Z.; Adams, E. M.; Allen, H. C. Cation Effects on Interfacial Water Organization of Aqueous Chloride Solutions. I. Monovalent Cations: Li^+, Na^+, K^+, and NH4$^+$. *J. Phys. Chem. B* **2014**, *118*, 8433−8440.
(44) Liu, D.; Ma, G.; Levering, L. M.; Allen, H. C. Vibrational Spectroscopy of Aqueous Sodium Halide Solutions and Air−Liquid Interfaces: Observation of Increased Interfacial Depth. *J. Phys. Chem. B* **2004**, *108*, 2252−2260.
(45) Yang, Z.; Li, Q.; Chou, K. C. Structures of Water Molecules at the Interfaces of Aqueous Salt Solutions and Silica: Cation Effects. *J. Phys. Chem. C* **2009**, *113*, 8201−8205.
(46) Du, Q.; Freysz, E.; Shen, Y. R. Vibrational Spectra of Water Molecules at Quartz/Water Interfaces. *Phys. Rev. Lett.* **1994**, *72*, 238−241.
(47) Ong, S.; Zhao, X.; Eisenthal, K. B. Polarization of Water Molecules at a Charged Interface: Second Harmonic Studies of the Silica/Water Interface. *Chem. Phys. Lett.* **1992**, *191*, 327−335.
(48) Stack, A. G.; Higgins, S. R.; Eggleston, C. M. Point of Zero Charge of a Corundum-Water Interface Probed With Optical Second Harmonic Generation (SHG) and Atomic Force Microscopy (AFM): New Approaches to Oxide Surface Charge. *Geochim. Cosmochim. Acta* **2001**, *65*, 3055−3063.
(49) Fitts, J. P.; Shang, X.; Flynn, G. W.; Heinz, T. F.; Eisenthal, K. B. Electrostatic Surface Charge at Aqueous/α-Al_2O_3 Single-Crystal Interfaces as Probed by Optical Second-Harmonic Generation. *J. Phys. Chem. B* **2005**, *109*, 7981−7986.
(50) Sauerbeck, C.; Braunschweig, B.; Peukert, W. Surface Charging and Interfacial Water Structure of Amphoteric Colloidal Particles. *J. Phys. Chem. C* **2014**, *118*, 10033−10042.
(51) Azam, M. S.; Weeraman, C. N.; Gibbs-Davis, J. M. Halide-Induced Cooperative Acid−Base Behavior at a Negatively Charged Interface. *J. Phys. Chem. C* **2013**, *117*, 8840−8850.
(52) Singh, P. C.; Nihonyanagi, S.; Yamaguchi, S.; Tahara, T. Interfacial Water in the Vicinity of a Positively Charged Interface

DOI: 10.1021/acs.jpcc.8b03004
J. Phys. Chem. C 2018, 122, 12819−12830

Studied by Steady-State and Time-Resolved Heterodyne-Detected Vibrational Sum Frequency Generation. *J. Chem. Phys.* **2014**, *141*, No. 18C527.
(53) Kropman, M. F.; Bakker, H. J. Effect of Ions on the Vibrational Relaxation of Liquid Water. *J. Am. Chem. Soc.* **2004**, *126*, 9135−9141.
(54) Kropman, M.; Bakker, H. Vibrational Relaxation of Liquid Water in Ionic Solvation Shells. *Chem. Phys. Lett.* **2003**, *370*, 741−746.
(55) Eftekhari-Bafrooei, A.; Borguet, E. Effect of Surface Charge on the Vibrational Dynamics of Interfacial Water. *J. Am. Chem. Soc.* **2009**, *131*, 12034−12035.
(56) Eftekhari-Bafrooei, A.; Borguet, E. Effect of Hydrogen-Bond Strength on the Vibrational Relaxation of Interfacial Water. *J. Am. Chem. Soc.* **2010**, *132*, 3756−3761.
(57) Eftekhari-Bafrooei, A.; Borguet, E. Effect of Electric Fields on the Ultrafast Vibrational Relaxation of Water at a Charged Solid−Liquid Interface as Probed by Vibrational Sum Frequency Generation. *J. Phys. Chem. Lett.* **2011**, *2*, 1353−1358.
(58) Ghorai, S.; Pant, K. K. Equilibrium, Kinetics and Breakthrough Studies for Adsorption of Fluoride on Activated Alumina. *Sep. Purif. Technol.* **2005**, *42*, 265−271.
(59) Loganathan, P.; Vigneswaran, S.; Kandasamy, J.; Naidu, R. Defluoridation of Drinking Water Using Adsorption Processes. *J. Hazard. Mater.* **2013**, *248*−*249*, 1−19.
(60) Vinati, A.; Mahanty, B.; Behera, S. K. Clay and Clay Minerals for Fluoride Removal from Water: A State-of-the-Art Review. *Appl. Clay Sci.* **2015**, *114*, 340−348.
(61) Bhatnagar, A.; Kumar, E.; Sillanpaa, M. Fluoride Removal from Water by Adsorption-A Review. *Chem. Eng. J.* **2011**, *171*, 811−840.
(62) Flörsheimer, M.; Kruse, K.; Polly, R.; Abdelmonem, A.; Schimmelpfennig, B.; Klenze, R.; Fanghänel, T. Hydration of Mineral Surfaces Probed at the Molecular Level. *Langmuir* **2008**, *24*, 13434−13439.
(63) DelloStritto, M.; Sofo, J. Bond Polarizability Model for Sum Frequency Generation at the $Al_2O_3(0001)/H_2O$ Interface. *J. Phys. Chem. A* **2017**, *121*, 3045−3055.
(64) Myalitsin, A.; Urashirna, S. H.; Nihonyanagi, S.; Yamaguchi, S.; Tahara, T. Water Structure at the Buried Silica/Aqueous Interface Studied by Heterodyne-Detected Vibrational Sum-Frequency Generation. *J. Phys. Chem. C* **2016**, *120*, 9357−9363.
(65) Sovago, M.; Campen, R. K.; Wurpel, G. W. H.; Muller, M.; Bakker, H. J.; Bonn, M. Vibrational Response of Hydrogen-Bonded Interfacial Water is Dominated by Intramolecular Coupling. *Phys. Rev. Lett.* **2008**, *100*, No. 173901.
(66) Boulesbaa, A.; Borguet, E. Vibrational Dynamics of Interfacial Water by Free Induction Decay Sum Frequency Generation (FID-SFG) at the Al_2O_3 (1120)/H_2O Interface. *J. Phys. Chem. Lett.* **2014**, *5*, 528−533.
(67) Leeuw, N. H.; Parker, S. C. Effect of Chemisorption and Physisorption of Water on the Surface Structure and Stability of Alpha-Alumina. *J. Am. Ceram. Soc.* **1999**, *82*, 3209−3216.
(68) Elam, J. W.; Nelson, C. E.; Cameron, M. A.; Tolbert, M. A.; George, S. M. Adsorption of H_2O on a Single-Crystal Alpha-Al_2O_3(0001) Surface. *J. Phys. Chem. B* **1998**, *102*, 7008−7015.
(69) Eng, P. J.; Trainor, T. P.; Brown, G. E.; Waychunas, G. A.; Newville, M.; Sutton, S. R.; Rivers, M. L. Structure of the Hydrated Alpha-Al_2O_3 (0001). *Science* **2000**, *288*, 1029−1033.
(70) Hass, K. C.; Schneider, W. F.; Curioni, A.; Andreoni, W. First-Principles Molecular Dynamics Simulations of H_2O on Alpha-Al_2O_3(0001). *J. Phys. Chem. B* **2000**, *104*, 5527−5540.
(71) Jena, K. C.; Covert, P. A.; Hore, D. K. The Effect of Salt on the Water Structure at a Charged Solid Surface: Differentiating Second- and Third-order Nonlinear Contributions. *J. Phys. Chem. Lett.* **2011**, *2*, 1056−1061.
(72) Isaienko, O.; Nihonyanagi, S.; Sil, D.; Borguet, E. Observation of the Bending Mode of Interfacial Water at Silica Surfaces by Near-Infrared Vibrational Sum-Frequency Generation Spectroscopy of the Stretch plus Bend Combination Bands. *J. Phys. Chem. Lett.* **2013**, *4*, 531−535.
(73) Kropman, M. F.; Bakker, H. J. Dynamics of Water Molecules in Aqueous Solvation Shells. *Science* **2001**, *291*, 2118−2120.
(74) Yeganeh, M.; Dougal, S.; Pink, H. Vibrational Spectroscopy of Water at Liquid/Solid Interfaces: Crossing the Isoelectric Point of a Solid Surface. *Phys. Rev. Lett.* **1999**, *83*, 1179.
(75) Miranda, P.; Xu, L.; Shen, Y.; Salmeron, M. Icelike Water Monolayer Adsorbed on Mica at Room Temperature. *Phys. Rev. Lett.* **1998**, *81*, 5876.
(76) Du, Q.; Freysz, E.; Shen, Y. R. Surface Vibrational Spectroscopic Studies of Hydrogen Bonding and Hydrophobicity. *Science* **1994**, *264*, 826−827.
(77) Gaigeot, M. P.; Sprik, M.; Sulpizi, M. Oxide/Water Interfaces: How the Surface Chemistry Modifies Interfacial Water Properties. *J. Phys.: Condens. Matter* **2012**, *24*, No. 124106.
(78) Smith, J. D.; Saykally, R. J.; Geissler, P. L. The Effects of Dissolved Halide Anions on Hydrogen Bonding in Liquid Water. *J. Am. Chem. Soc.* **2007**, *129*, 13847−13856.
(79) Mondal, J. A.; Nihonyanagi, S.; Yamaguchi, S.; Tahara, T. Structure and Orientation of Water at Charged Lipid Monolayer/Water Interfaces Probed by Heterodyne-Detected Vibrational Sum Frequency Generation Spectroscopy. *J. Am. Chem. Soc.* **2010**, *132*, 10656−10657.
(80) Bakker, H. J.; Kropman, M. F.; Omta, A. W. Effect of ions on the structure and dynamics of liquid water. *J. Phys.: Condens. Matter* **2005**, *17*, S3215.
(81) McGuire, J. A.; Shen, Y. R. Ultrafast Vibrational Dynamics at Water Interfaces. *Science* **2006**, *313*, 1945−1948.
(82) Smits, M.; Ghosh, A.; Bredenbeck, J.; Yamamoto, S.; Müller, M.; Bonn, M. Ultrafast Energy Flow in Model Biological Membranes. *New J. Phys.* **2007**, *9*, 390.
(83) Bonn, M.; Bakker, H. J.; Ghosh, A.; Yamamoto, S.; Sovago, M.; Campen, R. K. Structural Inhomogeneity of Interfacial Water at Lipid Monolayers Revealed by Surface-Specific Vibrational Pump−Probe Spectroscopy. *J. Am. Chem. Soc.* **2010**, *132*, 14971−14978.
(84) Lock, A.; Bakker, H. Temperature Dependence of Vibrational Relaxation in Liquid H_2O. *J. Chem. Phys.* **2002**, *117*, 1708−1713.
(85) Nienhuys, H.-K.; Woutersen, S.; van Santen, R. A.; Bakker, H. J. Mechanism for vibrational relaxation in water investigated by femtosecond infrared spectroscopy. *J. Chem. Phys.* **1999**, *111*, 1494−1500.
(86) Lock, A. J.; Woutersen, S.; Bakker, H. J. Ultrafast Energy Equilibration in Hydrogen-Bonded Liquids. *J. Phys. Chem. A* **2001**, *105*, 1238−1243.
(87) Ramasesha, K.; De Marco, L.; Mandal, A.; Tokmakoff, A. Water vibrations have strongly mixed intra- and intermolecular character. *Nat. Chem.* **2013**, *5*, 935−940.
(88) Marcus, Y. Effect of Ions on the Structure of Water: Structure Making and Breaking. *Chem. Rev.* **2009**, *109*, 1346−1370.
(89) Jungwirth, P.; Tobias, D. J. Specific Ion Effects at the Air/Water Interface. *Chem. Rev.* **2006**, *106*, 1259−1281.
(90) Tobias, D. J.; Stern, A. C.; Baer, M. D.; Levin, Y.; Mundy, C. J. Simulation and Theory of Ions at Atmospherically Relevant Aqueous Liquid-Air Interfaces. *Annu. Rev. Phys. Chem.* **2013**, *64*, 339−359.
(91) Kropman, M. F.; Nienhuys, H.-K.; Woutersen, S.; Bakker, H. J. Vibrational Relaxation and Hydrogen-Bond Dynamics of HDO: H_2O. *J. Phys. Chem. A* **2001**, *105*, 4622−4626.

DOI: 10.1021/acs.jpcc.8b03004
J. Phys. Chem. C 2018, 122, 12819−12830